Envelope-function approach for the electrodynamics of nonlinear periodic structures

C. Martijn de Sterke and J. E. Sipe
Department of Physics and Ontario Laser and Lightwave Research Centre, University of Toronto, Toronto, Ontario, Canada M5S 1A7
(Received 21 June 1988)

An envelope-function approach is used to give a theoretical description of the electromagnetic properties of nonlinear periodic structures. This method, in which the electric field is separated into slow and fast spatial components, shows that the slow field component satisfies the nonlinear Schrödinger equation. The well-known soliton solutions of this equation provide a theoretical description of the gap solitons found by Chen and Mills [Phys. Rev. Lett. **58**, 160 (1987)] in their numerical studies of these structures. The more general solutions of the nonlinear Schrödinger equation provide a framework for understanding the properties of finite nonlinear periodic stacks. Our method allows us to find these solutions analytically.

I. INTRODUCTION

The dispersion relations provide the key to understanding the electromagnetic properties of linear dielectric periodic thin-film stacks.[1,2] The solutions of the dispersion relations exhibit different branches, which are separated by stop gaps. No running wave solutions are allowed for radiation with a frequency falling within one of the stop gaps and, consequently, such radiation is strongly reflected.[1,2] This behavior is very similar to the energy bands and gaps for the electronic wave function in the theory of crystalline solids (see, e.g., Ref. 3). Recent work has shown that the introduction of an intensity-dependent refractive index in the dielectric stacks can change these properties dramatically.[4–8] The possibility of solitonlike behavior in such systems was mentioned by Winful in 1985.[4] Dispersion, which is necessary for the existence of solitons, is provided by the curvature of the branches of the dispersion relation. The constituent materials themselves need thus not be dispersive. An analysis of such a structure was published by Chen and Mills in 1987.[5,6] Their work, which is numerical in nature, shows that at certain intensities the transmissivity of the nonlinear stack can approach unity at frequencies in the stop gap, in sharp contrast to the properties of the highly reflective linear stack. The electric field profiles which Chen and Mills present indicate that the field has two components. The first of these varies on the scale of the individual layers of the stacks and is similar to the Bloch functions in solid-state physics. The second component varies on a much larger scale and acts as an envelope for the fast Bloch-like component. The numerical results of Chen and Mills seem to show that this slowly varying envelope can attain a solitonlike hyperbolic secant shape if the periodic structure is infinitely extended. To refer to such field profiles, which are associated with one of the stop gaps of the stack, Chen and Mills have introduced the term *gap soliton*.[5]

An approximate analytic description of this phenomenon was first given by Mills and Trullinger.[7] These authors only considered the special case of a sinusoidally varying dielectric function, in the limit in which the amplitude of that variation is small, and restricted themselves to harmonic fields. Essentially following the approach of Winful,[4] they derived equations for the slowly varying amplitudes of the two counterpropagating waves that are scattered into each other by the periodic inhomogeneity. Within their approximation, an envelope function of the total electric field is shown to satisfy the double-sine-Gordon equation,[7] which allows solitary-wave solutions. To lowest order, these have a hyperbolic secant shape, in agreement with the numerical work on these systems.[5,6] Mills and Trullinger only consider systems of infinite length, so that a matching procedure to the surrounding media is avoided.

Another analytic way of analyzing the previously mentioned structures was recently introduced by Sipe and Winful.[8] This approach, which is very general and is not confined to small index differences between the constituents, or even a particular form of the periodic dielectric function, leads to a differential equation for a slowly varying field amplitude as well. Here, however, the slowly varying amplitude modulates a Bloch function of the underlying periodic structure. Furthermore, the restriction to harmonic fields is not necessary. Sipe and Winful show that, within their approximation, the slow component satisfies the nonlinear Schrödinger equation. With appropriate boundary conditions, this equation allows soliton solutions.[9]

The major advantage of the analytic approaches[7,8] is that they focus on a slowly-varying envelope function, which is of primary physical interest. Compared to the method of Mills and Trullinger,[7] that of Sipe and Winful[8] is the more general, and it is the latter which is used in the present work. It allows us to characterize the periodic nonlinear stack by only a few parameters, avoiding the conventional description of the stack in terms of a piecewise continuous dielectric function completely. Furthermore, any periodic nonlinear structure can be treated with this approach. Restricting ourselves to electric fields with an harmonic time dependence, we show that the equation for the slow component of the field is identi-

cal to that for the electric field of a homogeneous nonlinear slab. In our approach, therefore, the nonlinear periodic stack is equivalent to an homogeneous slab of material. The fast Bloch-like, electric field component only enters the discussion in determining the parameters of the effective homogeneous stack and in making the connection with electric fields in the surrounding medium.

The method of Sipe and Winful[8] is based upon an asymptotic series expansion of the electric field. In the present paper we show that inclusion of only the leading term in this expansion will give rise to serious errors in calculating the energy flow of the system. For this reason, the first two terms in the series have to be included. To determine the transmissivity of a finite system, boundary conditions, of course, will have to be applied at the two boundaries of the stack. We show that, for all practical situations, the envelope function is essentially independent of the nonlinearity, close to the rear of the stack. This surprising result implies that in applying the boundary conditions at the rear surface of the stack, the nonlinearity may be neglected altogether. This allows us to find analytic expressions for the matching conditions, even for general nonlinear structures. As a result, the entire problem of the finite, nonlinear, periodic stack is solved, within the approximation, in analytic terms.

It should be mentioned that the procedure of Sipe and Winful[8] is quite similar to the effective-mass approximation (EMA) in solid-state physics,[10] in which the electronic wave function is separated into slow and fast components as well. To carry the analogy further, the solid-state structure which is most similar to the linear periodic stack is a semiconductor superlattice.[11] Application of the boundary conditions at the two end faces of the periodic stack is then equivalent to the application of the interface connection rules in the theory of superlattices. It should be noted that these boundary conditions can be applied exactly in the present problem, in sharp contrast to the situation in solid-state physics.[12] The envelope-function approach which we use presently differs in two important aspects from application of the EMA to superlattices. First, our approach must be based upon Maxwell's equations, whereas the EMA follows from the Schrödinger equation. Secondly, whereas the EMA has, as far as we know, only been applied to linear phenomena, our envelope approach is used to describe nonlinear effects as well.

In the present paper the name *stack* will refer to the periodic structure. This does not imply, however, that such structures can only be manufactured using vacuum-deposition techniques. At least in fiber geometries, it is possible to obtain periodic structures with a considerable number of periods by the interference of two counterpropagating laser beams.[13] Such a general periodic, effective one-dimensional structure is also amenable to the kind of analysis we present here. Another such structure would be a grated waveguide, where the variation in the thickness of the waveguide behaves, in leading to scattering of waveguide modes, such as a modulation in an effective dielectric constant.

The organization of this paper is as follows. Section II gives a derivation of the envelope-function equation. The formalism is then applied to infinite periodic structures in Sec. III. In Sec. IV we consider finite stacks but disregard the nonlinearity. The emphasis in this section is on the boundary conditions at the front and rear end of the stack. In Sec. V the full problem of the finite, nonlinear stack will be tackled. In Secs. IV and V the results of our approximation will be compared to numerical results. In Sec. VI we discuss some of the properties of the nonlinear stack and of our method of calculation. Finally, in the two appendixes we present some details of the calculations.

II. DERIVATION OF SLOWLY VARYING ENVELOPE EQUATIONS

The starting point of the derivation of the expressions for the slowly varying envelope function is the wave equation for the electric field. For a field, assumed to vary only as a function of the distance x along the stack, Maxwell's equations and the assumption of an isotropic dielectric function $\epsilon(x)$,

$$\mathbf{D}(x,t)=\epsilon(x)\mathbf{E}(x,t) , \tag{2.1}$$

lead to the result that $\mathbf{E}$ must lie in the (y,z) plane. We denote its amplitude by $E(x,t)$ and, for simplicity, treat the case of linear polarization. In adopting Eq. (2.1), where $\epsilon(x)$ is of course real, we neglect both absorption and intrinsic dispersion in the materials; these restrictions can easily be lifted if necessary. At this same level of approximation, the inclusion of an isotropic Kerr nonlinearity leads to an extra, nonlinear polarization in the same direction as $\mathbf{E}$, which is of the form[14]

$$P_{\mathrm{NL}}(x,t)=\chi^{(3)}(x)[E(x,t)]^3 , \tag{2.2}$$

where $\chi^{(3)}(x)$ is the nonlinear susceptibility. The inclusion of this nonlinear polarization in Maxwell's equations leads, in our geometry and using the "cgs system," to the wave equation[14]

$$-c^2\frac{\partial^2}{\partial x^2}E(x,t)+\epsilon(x)\frac{\partial^2}{\partial t^2}E(x,t)=-4\pi\frac{\partial^2}{\partial t^2}P_{\mathrm{NL}}(x,t) , \tag{2.3}$$

where c is the speed of light in vacuum. In this work we assume that $\epsilon(x)$ and $\chi^{(3)}(x)$ are both (real) periodic functions with the same period d. Except for satisfying this restriction, they are completely arbitrary.

Before considering the fully nonlinear problem, we first derive a key property of the electromagnetic modes of the linear periodic stack. We thus consider Eq. (2.3) with $P_{\mathrm{NL}}=0$ and look for stationary solutions. Setting

$$E(x,t)=\varphi_m(x)e^{-i\omega_m t}+\text{c.c.} , \tag{2.4}$$

where c.c. designates complex conjugation, we find that the φ_m must satisfy the eigenvalue equation

$$-c^2\frac{\partial^2}{\partial x^2}\varphi_m(x)=\epsilon(x)\omega_m^2\varphi_m(x) . \tag{2.5}$$

This equation is of the general Sturm-Liouville type and its eigenfunctions, therefore, must satisfy orthogonality

relations.[15] By applying periodic boundary conditions in the usual way,[15] these are found to be

$$\langle m \mid \epsilon \mid m' \rangle \equiv \int_0^L \varphi_m^*(x)\epsilon(x)\varphi_{m'}(x)dx = \delta_{m,m'} , \tag{2.6}$$

where L is the length over which the functions must be periodic. Note that the normalization conditions themselves, as well as the eigenfunctions φ_m, depend on the dielectric function $\epsilon(x)$. Although derived for the linear problem, Eq. (2.4) will be of primary importance in deriving the equations for the nonlinear periodic stack. Equation (2.5) has a different structure than the time-independent Schrödinger equation with a periodic potential, since the periodic "potential-like" function $\epsilon(x)$ multiplies the eigenvalue ω_m^2. One consequence of this is the form of the orthogonality relations, Eq. (2.6), which differ from the form familiar from quantum mechanics. Similarly, techniques based on the Schrödinger equation are not necessarily directly applicable to the present problem. An example of this is mentioned in Appendix A, where we derive expressions for the slope and for the curvature of the dispersion curves, for use later in this section.

Now return to the full nonlinear wave equation given by Eqs. (2.2) and (2.3). To find the solution for the slowly varying component of the field, we use the method of *multiple scales*.[9] This general technique calls in the present problem for the introduction of different length scales, $x_\alpha = \mu^\alpha x$ ($\mu \ll 1, \alpha = 0,1,2,\ldots$), and time scales, $t_\alpha = \mu^\alpha t$. It is important that in the subsequent discussion these new variables are considered to be independent. Under this condition, the first spatial and temporal derivatives can be written as

$$\frac{\partial}{\partial x} = \frac{\partial}{\partial x_0} + \mu\frac{\partial}{\partial x_1} + \mu^2\frac{\partial}{\partial x_2} + \cdots , \tag{2.7}$$

and

$$\frac{\partial}{\partial t} = \frac{\partial}{\partial t_0} + \mu\frac{\partial}{\partial t_1} + \mu^2\frac{\partial}{\partial t_2} + \cdots , \tag{2.8}$$

from which expressions for higher derivatives follow straightforwardly. Similarly, the electric field E is written in a series

$$E = \mu e_1 + \mu^2 e_2 + \mu^3 e_3 + \cdots . \tag{2.9}$$

The e_i are functions of all x_α and all t_α, but these arguments will not be written explicitly. In taking ϵ and $\chi^{(3)}$ to be strictly periodic, we assume that they show variation only on the smallest length scale $\epsilon = \epsilon(x_0)$, $\chi^{(3)} = \chi^{(3)}(x_0)$. Equations (2.7), (2.8), and (2.9) are now substituted into Eqs. (2.2) and (2.3) and terms with equal powers of μ are collected. This substitution results in equations for the ϵ_i in the asymptotic expansion of Eq. (2.9). In the present paper, terms containing at most cubic terms in μ will be considered.

As a first step we gather all terms proportional to μ and find

$$\left[-c^2\frac{\partial^2}{\partial x_0^2} + \epsilon(x_0)\frac{\partial^2}{\partial t_0^2}\right] e_1 = 0 . \tag{2.10}$$

This equation, which is just the linear wave equation, shows that the nonlinearity plays no role on the fastest spatial and temporal time scales. From the analysis earlier in this section we know that the functions in Eq. (2.4) are solutions to this equation. Notice, however, that Eq. (2.10) only contains the variables x_0 and t_0, so that e_1 can be written as

$$e_1 = a(x_1,x_2,\ldots;t_1,t_2,\ldots)\varphi_m(x_0)e^{-i\omega_m t_0} + \text{c.c.} \tag{2.11}$$

In this equation, $a(x_1,x_2,\ldots;t_1,t_2,\ldots) \equiv a(x_i;t_i)$, where the subscript i runs over all positive integers, is an arbitrary function of the slow variables. This freedom will be limited by the subsequent analysis involving terms with higher orders in μ. Because $a(x_i;t_i)$ is a function of the slow variables only, we refer to it and to functions with this same property as *envelope functions*.

Next, we consider all terms proportional to μ^2 and find

$$\left[-c^2\frac{\partial^2}{\partial x_0^2} + \epsilon(x_0)\frac{\partial^2}{\partial t_0^2}\right] e_2 = \left[2c^2\frac{\partial}{\partial x_0}\frac{\partial}{\partial x_1} - 2\epsilon(x_0)\frac{\partial}{\partial t_0}\frac{\partial}{\partial t_1}\right] e_1 . \tag{2.12}$$

In order to solve this equation we make the following ansatz for e_2:

$$e_2 = \sum_l b_l(x_1,x_2,\ldots;t_1,t_2,\ldots)\varphi_l(x_0)e^{-i\omega_m t_0} + \text{c.c.} , \tag{2.13}$$

where the $b_l(x_i;t_i)$ are a new set of envelope functions. Substituting Eq. (2.13) into Eq. (2.12), we find

$$\sum_l (\omega_l^2 - \omega_m^2)\epsilon\varphi_l b_l = 2i\left[c(\Omega\varphi_m)\frac{\partial a}{\partial x_1} + \omega_m\epsilon\varphi_m\frac{\partial a}{\partial t_1}\right] , \tag{2.14}$$

where the arguments are not written explicitly and where the operator Ω is defined as

$$\Omega = -ic\frac{\partial}{\partial x_0} . \tag{2.15}$$

The quite complicated expression in Eq. (2.14) will be analyzed in two stages. In the first of these we project onto the subspace spanned by the eigenfunction φ_m. The left-hand side of Eq. (2.14) then vanishes and the following condition for envelope function $a(x_i;t_i)$ is found:

$$c\langle m \mid \Omega \mid m \rangle\frac{\partial a}{\partial x_1} + \omega_m\frac{\partial a}{\partial t_1} = 0 , \tag{2.16}$$

where the orthogonality relations in Eq. (2.6) were used. From Eq. (A9) of Appendix A, we see that the multiplying factors in Eq. (2.16) can be rewritten in terms of the group velocity ω_m' at the point on the dispersion curve associated with the state φ_m. It then follows that, in order to satisfy Eq. (2.16), the slowly varying function $a(x_i;t_i)$ cannot depend on x_1 and t_1 independently but only on the linear combination

$$z_1 \equiv x_1 - \omega_m' t_1 \ . \tag{2.17}$$

This brings us to the important conclusion that, to this level of approximation, the envelope travels with the group velocity. This conclusion reflects the fact that neither the nonlinearity nor the dispersion of the stationary states [Eq. (2.4)] have entered the discussion yet. Equation (2.16) [and (2.22), to be derived later] is known as an *asymptotic solvability condition*.[9] If it were not satisfied, it is easy to see that e_2 would diverge asymptotically as $t \to \infty$, contrasting the assumption that succeeding terms in Eq. (2.9) are smaller for all times.

In the next stage of analyzing Eq. (2.14) we project onto the space spanned by the remaining eigenfunctions φ_l $(l \neq m)$. Using the orthogonality relations [Eq. (2.6)] again, we now find an expression for the $b_l(x_i;t_i)$ in terms of the envelope function $a(x_i;t_i)$. It reads

$$b_l(x_1,x_2,\ldots;t_1,t_2,\ldots) = \frac{\partial a}{\partial z_1} \Lambda_{l,m} d \ , \tag{2.18}$$

where d is the period of the stack and the coupling coefficient $\Lambda_{l,m}$ is defined as

$$\Lambda_{l,m} = \frac{2ic}{d} \frac{\langle l \mid \Omega \mid m \rangle}{\omega_l^2 - \omega_m^2} \ . \tag{2.19}$$

The definition in Eq. (2.19) assures that the coupling coefficient is dimensionless. It follows from these expressions that the envelopes $b_l(x_i;t_i)$ travel with the group velocity as well.

Now we finally collect all the terms proportional to μ^3. The rather lengthy result can be written as

$$\left[-c^2 \frac{\partial^2}{\partial x_0^2} + \epsilon(x_0) \frac{\partial^2}{\partial t_0^2} \right] e_3 = \mathcal{F} \ , \tag{2.20}$$

where $\mathcal{F}$ is defined as

$$\begin{aligned} \mathcal{F} = & -4\pi \chi^{(3)} \frac{\partial^2}{\partial t_0^2} (e_1^3) \\ & + \left[c^2 \left(\frac{\partial^2}{\partial x_1^2} + 2 \frac{\partial}{\partial x_0} \frac{\partial}{\partial x_2} \right) \right. \\ & \left. - \epsilon(x_0) \left(\frac{\partial^2}{\partial t_1^2} + 2 \frac{\partial}{\partial t_0} \frac{\partial}{\partial t_2} \right) \right] e_1 \\ & + 2 \left[c^2 \frac{\partial}{\partial x_0} \frac{\partial}{\partial x_1} - \epsilon(x_0) \frac{\partial}{\partial t_0} \frac{\partial}{\partial t_1} \right] e_2 \ . \end{aligned} \tag{2.21}$$

It is thus only at this level that the nonlinearity explicitly enters the discussion. Like the analysis of Eq. (2.12), that of Eq. (2.20) should also take place in two stages. However, for the current purposes it is sufficient to project onto the subspace spanned by φ_m only. Using a similar ansatz as Eq. (2.13) it can be shown that the left-hand side of Eq. (2.20) is orthogonal to φ_m. The right-hand side of Eq. (2.20) will then provide another asymptotic solvability condition for the envelope function $a(x_i;t_i)$. We thus left multiply $\mathcal{F}$ by φ_m^* and integrate. After some algebraic manipulations, the result is then

$$\begin{aligned} 0 = & 2i\omega_m \left[\frac{\partial a}{\partial t_2} + \omega_m' \frac{\partial a}{\partial x_2} \right] + \omega_m'' \omega_m \frac{\partial^2 a}{\partial z_1^2} \\ & + a^* a^2 \left[12\pi \omega_m^2 \int_0^L \chi^{(3)}(x_0) \mid \varphi_m(x_0) \mid^4 dx_0 \right] \ , \end{aligned} \tag{2.22}$$

where we have used Eq. (A10) from Appendix A for the group-velocity dispersion ω_m'' at the point on the dispersion curve associated with the state φ_m.

In the remainder of this section we rewrite Eq. (2.22) in a more practical form. To do so, we note that ultimately we want to let $\mu \to 1$. Then if we interpret z_1 as our (slow) spatial coordinate (in the frame moving with the group velocity) we look for solutions for which $\partial/\partial x_2 = 0$. As $\mu \to 1$ then t_2 can be identified as "the" (slow) time.

Defining

$$a(x_i;t_i) = \sqrt{L}\, \bar{a}(x_i;t_i) \ , \tag{2.23}$$

and using the definition of the spatial and temporal coordinates from the previous paragraph, Eq. (2.22) can be rewritten as[8]

$$i \frac{\partial \bar{a}}{\partial t_2} + \tfrac{1}{2} \omega_m'' \frac{\partial^2 \bar{a}}{\partial z_1^2} + \alpha_m \mid \bar{a} \mid^2 \bar{a} = 0 \ , \tag{2.24}$$

where

$$\alpha_m = 6\pi \omega_m L \int_0^L \chi^{(3)}(x_0) \mid \varphi_m(x_0) \mid^4 dx_0 \ . \tag{2.25}$$

This coefficient represents the effective nonlinearity seen by the envelope function, and it depends on the way the fast Bloch-like component samples the optical nonlinearity. The definition in Eq. (2.25) assures that α_m is independent of the normalization length L.

From Eq. (2.24) we see that $\bar{a}(z_1,t_2)$ satisfies the nonlinear Schrödinger equation.[9] Since it plays an important role in many nonlinear phenomena, this equation and its solutions have been widely studied, and that body of knowledge can now be brought to bear in understanding the propagation of light through a nonlinear periodic medium. One of the best known properties of the nonlinear Schrödinger equation is the existence of soliton solutions;[9] we encounter these in Sec. III.

Knowledge of the slowly varying envelope $\bar{a}(z_1;t_2)$, together with Eqs. (2.11), (2.13), (2.17), (2.18), (2.19), and (2.23), completely determines the first two terms in the asymptotic expansion, Eq. (2.9). In the subsequent discussion, the total electric field will be approximated by the sum of these two terms; e_3 and higher-order terms will thus be neglected. Consequently, e_1 and e_2 play a very prominent role, and to reflect this we refer to these terms as the *principal* term and the *companion* term, respectively. From the definitions [Eqs. (2.11) and (2.13)], both consist of products of envelope functions and Bloch functions. For the remainder of the present paper we further drop the subscripts of z_1 and t_2 and we suppress all coordinates x_n and t_n for $n \geq 3$, so that $\bar{a} = \bar{a}(z,t)$.

III. STATIONARY SOLUTIONS IN AN INFINITE STACK

Although the derivation in Sec. II applies to fields of rather arbitrary space and time dependence, in this paper we hereafter restrict ourselves to strictly monochromatic electromagnetic fields with envelope functions that are at rest in space. We refer to such solutions as *stationary*. These form the simplest nontrivial class of solutions to Eq. (2.24), and, as we will see in Sec. IV, are important in understanding the transmission of a finite stack at frequencies in the (linear) stop gap. In particular, we can make a connection with the work of Chen and Mills:[5,6] we show below that the stationary solitons of the present theory form an analytic description of the *gap solitons* found numerically by those authors.

Since, as we saw in Sec. II, the envelope travels with the group velocity, our stationary solutions must be built on Bloch functions for which the group velocity vanishes. This implies that φ_m is either in the middle or at the edge of the Brillouin zone of the periodic stack (see Fig. 1). In the present paper we chose the latter, which allows us to make a direct comparison with the work of Chen and Mills.[5,6] Moreover, it assures us access to the lowest and, in general, widest stop gap. The conservation law of crystal momentum[3] tells us that, in the summation over l in Eq. (2.13), we only have to include eigenstates which are positioned at the Brillouin zone edge as well. Such eigenfunctions have some rather special properties: the vanishing of the group velocity implies that no energy is being transported, and the eigenfunctions are thus standing waves and can be chosen to be real. Also, as seen from Fig. 1, the eigenfunctions will border a stop gap; φ_m and each of the φ_l will thus make up either the lower edge, or the upper edge of a stop gap. Finally, all eigenfunctions will have a definite parity. Because the group velocity ω_m' vanishes, we can put $z=x$ in Eq. (2.24).

Furthermore, since we wish to treat monochromatic electric fields, we seek envelope functions of the form

$$\bar{a}(x,t)=\psi(x)e^{-i\delta t} . \tag{3.1}$$

Equations (2.11), (2.13), and (3.1) show that the resulting electric field indeed has harmonic time dependence with angular frequency $\omega_m+\delta$. Since, in the linear limit, the Bloch function being modulated has an eigenfrequency ω_m, we refer to δ as the *detuning*. Substituting Eq. (3.1) into the nonlinear Schrödinger equation leads to an equation for ψ,

$$\tfrac{1}{2}\omega_m''\frac{d^2\psi}{dx^2}+\delta\psi+\alpha_m|\psi|^2\psi=0 . \tag{3.2}$$

To cast Eq. (3.2) in its final form, we define the two parameters A and B by

$$A=\sqrt{-2\delta/\alpha_m} , \tag{3.3a}$$

$$B=\sqrt{-2\delta/\omega_m''} . \tag{3.3b}$$

We comment below on the sign under the radicals in Eqs. (3.3). Expressed in these two parameters we then find that

$$\frac{d^2\psi}{dx^2}-B^2\psi+2\frac{B^2}{A^2}|\psi|^2\psi=0 . \tag{3.4}$$

This equation for the envelope function is a significant simplification compared to the equation for the entire field. The necessary information regarding the refractive indices and the thicknesses of the constituent layers are "hidden" in the parameters A and B. To get an idea of the nature of this simplification, we return to Eqs. (2.2) and (2.3) for the total electric field. Let us rewrite this equation for the special case of an homogeneous medium, and, just as in deriving Eq. (3.4), only consider stationary solutions in time. Under these restrictions, Eqs. (2.2) and (2.3) take the form

$$\frac{d^2E_0}{dx^2}+k^2E_0+\frac{12\pi\chi^{(3)}}{\epsilon}k^2|E_0|^2E_0=0 , \tag{3.5}$$

where k is the wave vector of the radiation inside the medium, and third harmonic generation was neglected. We thus see that the equation for the envelope function of the electric field associated with the nonlinear stack [Eq. (3.4)], is equivalent to that for the total field of a nonlinear homogeneous medium [Eq. (3.5)]. As far as the envelope is concerned, therefore, the nonlinear stack behaves as a homogeneous slab, characterized by A and B only.

We now return to the choice of the signs under the radicals in Eqs. (3.3). These signs have been chosen in such a way that A and B are real for the situations of main interest. Let us first consider the limit in which $A\to\infty$, which, according to Eqs. (3.4) and (3.3a) corresponds to the case in which the nonlinearity vanishes. For the parameter B to be real, Eq. (3.3b) prescribes that δ and ω_m'' should have opposite signs. Figure 1 shows that, because φ_m is at the edge of the Brillouin zone, the radiation is at a frequency which lies in the stop gap of the stack. This is consistent with Eq. (3.4) since, in the linear limit, the envelope function consists of an exponentially growing and decaying part. This is exactly the kind of behavior to be expected for radiation tuned to a stop gap. The inverse of B can be interpreted as the associated decay length [Eq. (3.4)]. The envelope function is thus

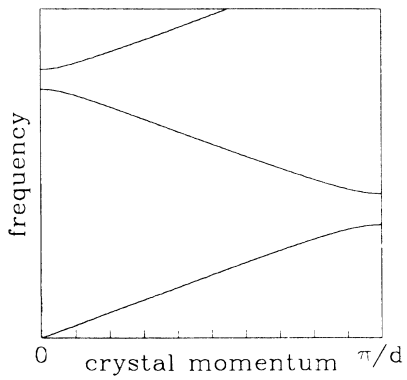

FIG. 1. Schematic of dispersion curve of a periodic dielectric stack in the reduced zone scheme.

slowly varying if this decay length is much larger than the period d of the constituents of the stack, or when

$$1/(Bd) \gg 1 \ . \tag{3.6}$$

In the linear limit, the stack thus behaves as a homogeneous medium with an imaginary wave vector, e.g., as a conductor without dissipation.

Now consider finite values for the parameter A. From Eq. (3.4), we only expect significant changes compared to the behavior in the linear limit when the second and the third terms have opposite signs. Thus, when A is imaginary, the only effect of the nonlinearity will be to make the decay length even shorter. For real A, on the other hand, we see that if $|\psi| \approx A$, the second derivative of the envelope function will change sign, so that, locally, the stack behaves as a medium with real refractive index. The reason for this behavior can be seen from Eq. (3.3a). For A to be real, α_m and δ should have opposite signs, which, by Eq. (2.25), means that $\chi^{(3)}$ and δ should have opposite sign. A negative value of $\chi^{(3)}$ will tend to decrease the refractive indices, and, consequently, will tend to shift the stop gap to higher energies for large intensities for negative $\chi^{(3)}$. Since $\chi^{(3)}$ and δ have opposite signs, this means that at high intensities the incoming light is shifted towards the nearest band edge. For sufficiently high intensities this shift can exceed the detuning so that the radiation "leaves" the stop gap. At these high intensities running wave solutions of the envelope function will thus be allowed.

Before discussing solutions of Eq. (3.4) it is useful to have a general expression for the electric field in terms of the envelope function ψ. Using Eqs. (3.1), (2.23), (2.11), (2.13), and (2.18) we find that

$$E(x,t) = E_0(x) e^{-i\omega t} + \text{c.c.} \ , \tag{3.7}$$

where

$$E_0(x) = \psi(x)[\sqrt{L}\,\varphi_m(x)] + \sum_{l\,(\neq m)} (Bd)\Lambda_{l,m} \left[\frac{1}{B}\frac{d\psi}{dx}\right][\sqrt{L}\,\varphi_l(x)] \ , \tag{3.8}$$

where the distinction between the slow and the fast variables was dropped. According to the nomenclature introduced at the end of Sec. II, the first term on the right-hand side is the principal term, whereas the second is the companion term. We now compare the sizes of these two contributions. To do this, we estimate the size of the multiplying factors of the Bloch functions in this equation. Since the envelope function ψ varies over a length scale of about $1/B$, the third multiplying factor in the second term in Eq. (3.8) is thus in general of the same order as ψ. But because of Eq. (3.6) the product of the coupling parameter $\Lambda_{l,m}$ and (Bd) is much smaller than unity. This is true even when $\omega_m \approx \omega_l$ [see Eq. (2.19)]; the demonstration follows straightforwardly from the definitions of the parameters involved and relies on the fact that the envelope function approach is only valid when $\delta \ll |\omega_l - \omega_m|$. This result is shown to be true in Sec. VI. We thus conclude that the principal term dominates the electric field, as expected. This does not mean that the companion term can be neglected altogether, however, as becomes clear if we calculate the energy flow associated with the electric field in Eq. (3.7). From the definition and from Maxwell's equations we find, for the time- and space-averaged Poynting vector,

$$\langle S \rangle_{x,t} = \frac{c^2}{2\pi\omega} \mathrm{Im}\left\langle E_0^* \frac{dE_0}{dx} \right\rangle_x \ , \tag{3.9}$$

where the subscripts indicate to the average being taken, and the spatial average refers to a period of the stack. The subscripts will henceforth be dropped. Substituting Eq. (3.8) into this equation and neglecting terms proportional to $\Lambda_{l,m}^2$, the result is

$$\langle S \rangle = \frac{c^2}{2\pi\omega} \times \mathrm{Im}\left\{ \psi^* \psi' \langle m \mid m \rangle + \sum_{l\,(\neq m)} d\Lambda_{l,m} \left[\left\{ \frac{i}{c} \psi^* \psi' \langle m \mid \Omega \mid l \rangle + \text{c.c.} \right\} + \psi^* \psi'' \langle m \mid l \rangle \right] \right\} , \tag{3.10}$$

with the operator Ω defined in Eq. (2.15). Furthermore, use was made of the fact that the Bloch functions at the Brillouin zone edge can be chosen to be real, and that they vary on a much faster scale than the envelope function. Note that the contribution to $\langle S \rangle$ from the term containing the product $\psi^* \psi \varphi_m^* \varphi_m'$ vanishes. We would normally have expected this term, with the derivative of the Bloch function, to dominate in Eq. (3.10), since the Bloch functions vary on a length scale d, while the envelope functions vary on a scale $1/B$, and thus

$$\left| \frac{d\psi}{dx} \Big/ \frac{d\varphi_m}{dx} \right| = O(Bd) \ll 1 \tag{3.11}$$

[see Eq. (3.6)]. But because we have chosen a Bloch function at a point on the dispersion curve where the group velocity vanishes, the Bloch function can be chosen real and $\mathrm{Im}(\psi^* \psi \varphi_m^* \varphi_m') = 0$. Physically, such a Bloch function corresponds to a standing wave and cannot itself contribute to the energy flow; such a flow must appear from the envelope functions, and thus the largest nonvanishing contributions to the energy flow are the terms in Eq. (3.10).

The first of the terms in Eq. (3.10) contains the derivative of the envelope function in the principal term in Eq. (3.8), whereas the second contains the derivative of the Bloch function in the companion term in this equation. We thus have the somewhat surprising result that the energy flow involving the companion term in Eq. (3.8) can be as large as, and will often be larger than, the energy flow associated with the principal term in this equation only. In fact, in some practical situations, the second term in Eq. (3.10) is larger than the first term and has opposite sign; if one only included the principal term in the

expression for the electric field, one would predict an energy flow in the wrong direction. It is clear that the second term in Eq. (3.8) is thus crucial for a correct description of the electric field.

The last term in Eq. (3.10) will be neglected, as it contains a derivative of an envelope function rather than that of a Bloch function: this, by Eq. (3.11), is equivalent to an extra factor (Bd). Using Eq. (A10), the leading term in the expression for the energy flow can thus be written as

$$\langle S \rangle = \frac{\omega_m''}{2\pi} \mathrm{Im}(\psi^* \psi') \ . \tag{3.12}$$

The occurrence of the group-velocity dispersion in this equation might at first seem surprising. It is somewhat similar to the occurrence of the effective mass in elementary expressions for the electrical conductivity of solids. These prescribe that the conductivity is inversely proportional to the effective mass, and thus proportional to the curvature of the energy bands (be it positive or negative). Furthermore, in order to transfer energy, the slowly varying envelope function gives access to the immediate neighborhood of the band edge. The information regarding the group velocity in this region is, to lowest order, provided for by ω_m''.

After these preliminaries we are now in the position to solve Eq. (3.4) and to interpret the results. We first neglect the nonlinearity by taking the limit in which $A \to \infty$. Equation (3.4) can then solved by inspection,

$$\psi_L = Pe^{Bx} + Qe^{-Bx} \ , \tag{3.13}$$

where P and Q are constants; this is not unexpected for radiation corresponding to the stop gap of a periodic structure, as discussed at the beginning of this section. Using Eqs. (3.7) and (3.8) the entire electric field can then be found; this gives

$$E_0(x) = (Pe^{Bx} + Qe^{-Bx})[\sqrt{L}\,\varphi_m(x)] + \sum_{l \neq m} (Bd)\Lambda_{l,m}(Pe^{Bx} - Qe^{-Bx})[\sqrt{L}\,\varphi_l(x)] \ . \tag{3.14}$$

To finish this survey of the properties of the linear stack, let us calculate the crucial quantity $\mathrm{Im}(\psi^* \psi')$, which appears Eq. (3.12) for the energy flow. Using Eq. (3.13) we find immediately that

$$\mathrm{Im}(\psi^* \psi') = 2B \ \mathrm{Im}(PQ^*) \ . \tag{3.15}$$

This expression will be used extensively in subsequent sections. It should be stressed at this point that Eq. (3.13) represents the full formal solution to the linear problem in its most general form. For a semi-infinite stack, for example, the exponentially growing term vanishes, and so, by Eq. (3.15), does the energy flow.

Now consider solutions of (Eq. 3.14) for finite values of the parameter A. It was mentioned before that, as far as the envelope function is concerned, the stack is equivalent to a homogeneous slab of material [Eqs. (3.4) and (3.5)]. The properties of a single homogeneous nonlinear slab have been presented,[16] and we can apply the method straightforwardly to the present problem. For this reason, only the results of this derivation will be given; the reader is referred to the literature[16] for details. First, the envelope function is written as

$$\psi(x) = \mathcal{E}(x) e^{i\phi(x)} \ , \tag{3.16}$$

where $\mathcal{E}(x)$ and $\phi(x)$ are real functions. Instead of working with $\mathcal{E}$ it is more convenient to introduce the function $I(x)$,

$$I(x) = \mathcal{E}^2(x) \ , \tag{3.17}$$

in terms of which the phase factor $\phi(x)$ is given by

$$\phi(x) = W \int^x \frac{1}{I(x')} dx' \ . \tag{3.18}$$

By Eqs. (3.16)–(3.18), the envelope function $\psi(x)$ is completely determined by $I(x)$. The expression for $I(x)$ is

$$I(x) = I_+ - (I_+ - I_m)\mathrm{sn}^2 \left[\sqrt{I_+ - I_-}\, \frac{B}{A} x \,\middle|\, k \right] , \tag{3.19}$$

where $\mathrm{sn}(x)$ is one of the Jacobi elliptic functions.[17,18] The modulus k of the elliptic function[19] is given by the expression

$$k = \left[\frac{I_+ - I_m}{I_+ - I_-} \right]^{1/2} \ . \tag{3.20}$$

Finally, the parameters I_+ and I_- are defined by

$$I_\pm = \frac{1}{2} \left[A^2 - I_m \pm \left[(A^2 - I_m)^2 + \frac{4W^2 A^2}{I_m B^2} \right]^{1/2} \right] . \tag{3.21}$$

The free parameters in these equations are I_m and W. The latter, however, has a simple interpretation, which becomes clear if we calculate $\mathrm{Im}(\psi^* \psi')$. Using Eqs. (3.16)–(3.18), it follows immediately that

$$\mathrm{Im}(\psi^* \psi') = W \ , \tag{3.22}$$

and thus, by Eq. (3.12), that the energy flow is proportional to W. The parameter W is thus fixed by the Poynting vector. The parameter I_m does not have such a simple interpretation and it will have to be chosen in accordance with the boundary conditions.

Since the elliptic function $\mathrm{sn}(x)$ varies periodically between -1 and $+1$ for real arguments, we conclude that $I(x)$ varies periodically between I_+ and I_m. Because of the definition of the function $I(x)$, Eq. (3.17), I_m must thus be positive. Now turn to the relative sizes of the parameters I_m, I_+, and I_-. It can be seen from Eqs. (3.21) that I_+ is always positive and that I_- is negative or zero. Both can be found as a complicated function of I_m. In all practical situations, I_+ is larger than I_m, so that $I_+ \geq I_m \geq I_-$. The modulus k [Eq. (3.20)] thus lies between zero and unity. Because $\mathrm{sn}(0) = 0$, it is found from Eq. (3.19) that $I(0) = I_+$. It will be useful in Sec. V to have an expression for $I(x)$ such that $I(0) = I_m$. By using the properties of the elliptic functions,[17,18] we can shift the origin such that

$$I(x)=I_+-(I_+-I_m)\mathrm{cd}^2\left[\sqrt{I_+-I_-}\,\frac{B}{A}x\,\middle|\,k\right], \quad (3.23)$$

where $\mathrm{cd}(x)$ is another of the Jacobi elliptic functions, which also varies between -1 and $+1$. Since $\mathrm{cd}(0)=1$, Eq. (3.23) has the desired property. In Sec. V we will investigate the preceding expressions in detail.

We will presently make the connection with the numerical work of Chen and Mills.[5,6] To do this, we consider a limiting case of the foregoing equations. First we let the energy flow vanish, which implies that $W=0$, and we then take the limit in which $I_m\to 0$. Equations (3.21) then yield that $I_+=A^2$ and $I_-=0$, so that, using Eq. (3.20), the modulus $k=1$. The elliptic function $\mathrm{sn}(x)$ is identical to $\tanh(x)$ for this special value of the modulus. The envelope function now attains the standard soliton shape[9]

$$\psi(x)=A\,\mathrm{sech}(Bx)\ . \quad (3.24)$$

The total electric field can now be found using Eqs. (3.7) and (3.8). The envelope function in Eq. (3.24) represents a soliton which has the unique property of being at rest in space. Since we have set $W=0$, this soliton does not transfer energy. In order to do this, it would have to be perturbed, by changing W and I_m appropriately. It should be stressed that such behavior is quite common for resonances in a cavity.[20] Notice, however, that in the present situation this behavior occurs in an infinite medium. We return to this matter in Sec. V.

To finish this section we now compare the properties of the gap solitons found by Chen and Mills[5,6] in their numerical studies, with analytic expressions for the electric field associated with the envelope function in Eq. (3.24). For the qualitative comparisons we do here, we need only consider the principal term in Eq. (3.8). Chen and Mills mention that their numerical work suggests that gap solitons have the following three characteristic properties. First, the product of $\chi^{(3)}$ and the peak intensity is constant. By Eqs. (3.3a) and (2.25), the soliton described by Eq. (3.24) has this same property. Secondly, Chen and Mills find that the width is independent of $\chi^{(3)}$. By Eqs. (3.3b) and (3.24) we come to the same conclusion. Thirdly, for positive (negative) values of $\chi^{(3)}$ they only find solutions near the upper (lower) edge of a stop gap. Again, we reach the same conclusion from Eq. (3.3a). We can thus be confident that our formalism is qualitatively consistent with numerical results.[5,6] In Secs. IV–VI the properties of the nonlinear stack will be investigated in much more detail and the results will be checked in a quantitative manner.

IV. LINEAR FINITE STACK

We now turn our attention to structures of finite length. Here, the differential equation governing the electromagnetic field inside and outside the structure have to be solved subject to the appropriate boundary conditions at $|x|\to\infty$, as well as the Maxwell saltus condition at the interfaces between the outside medium and the structure. In the present section we only consider the linear problem; the more general, nonlinear case will be discussed in Sec. V. Of course, we are not suggesting that the envelope-function approach is a useful method for treating the linear stack. The exact results in this case are too easily found and are too well understood to merit the use of an approximate method. Rather, the envelope-function approach will prove to be far more useful in treating the nonlinear stack. The difficulty of the general problem there does justify the use of an approximate method, which can provide more physical insight than fully numerical calculations. There are, however, two reasons for first discussing the linear stack in the envelope-function approach. First, it allows us to use the simpler case as a benchmark to judge the severity of our approximations. Further, we show in Sec. V that, in all situations in which the envelope function approach is applicable, the interface conditions on the envelope function for the linear and for the nonlinear stack are identical. The results from the present section are thus directly applicable to the nonlinear problem.

We thus now assume that the stack has a finite length and that the equations from Secs. II and III apply inside. The surrounding medium is assumed to be homogeneous, linear, and loss free, and we put the rear of the stack at $x=0$. We will match the electric field inside the stack to a plane wave in the surrounding medium. As in all such problems, the analysis starts at the rear surface of the structure, since only an outgoing wave will be present here, and it is then continued by integrating forward in the stack.[1,2] At this point, the advantages of the envelope approach become clear, since the envelope function allows us to jump immediately to the front end of the stack, no matter how long it is. This should be contrasted to the conventional methods where the integration has to be done layer by layer. Note the different footing of the front and the back surface of the structure: the electric field inside the stack is uniquely determined by the fact that at the rear surface one only has an outgoing wave (with given wavelength). The position of the front surface only determines how far one has to integrate forward, and, in this way, influences the transmissivity of the stack. It does not influence the field within the structure, however.

To satisfy the boundary conditions we have to know the electric field as a whole; knowledge of just the envelope function will not suffice. For the linear stack we thus use Eq. (3.14). Once the origin of the x coordinate has been chosen, this is a linear equation in P and Q. The coefficients in this equation depend on the details of the Bloch functions, but can be certainly be calculated. It is easily verified from Maxwell's equations that matching the transverse component of the magnetic field across the interface in the present geometry is equivalent to matching dE/dx. The latter, from Eq. (3.14), will also be a linear function in P and Q. By equating Eq. (3.14) and its first derivative to the electric field associated with a plane wave, therefore, the coefficients P and Q can be found (once the origin of the x coordinate has been fixed). It should be mentioned that in this procedure only the values of the Bloch functions and their first derivatives at the interface are required. To be more concrete, using the expressions for the total electric field, Eqs. (3.7) and (3.14), and its first derivative, we find

$$\begin{bmatrix} E(0) \\ E'(0) \end{bmatrix} = \begin{bmatrix} m_0 & \sum (Bd)\Lambda_{l,m} l_0 \\ m'_0 + B \sum (Bd)\Lambda_{l,m} l_0 & Bm_0 + \sum (Bd)\Lambda_{l,m} l'_0 \end{bmatrix} \begin{bmatrix} P+Q \\ P-Q \end{bmatrix}, \tag{4.1}$$

where we have made use of the following notation:

$$\begin{aligned} m_0 &= \sqrt{L}\,\varphi_m(0)\ , \\ m'_0 &= \sqrt{L}\,\varphi'_m(0)\ , \end{aligned} \tag{4.2}$$

and similarly for φ_l. The summation in this equation, and in subsequent ones, includes all states $l \neq m$. Since the origin in Eq. (4.1) is taken at the rear surface of the stack, the quantities defined in Eq. (4.2) refer to the Bloch functions and their derivate at that position only. In matching to an outgoing plane wave these will be fixed, apart from an unimportant overall phase factor, by the wavelength, and by the energy flow [see Eq. (3.9)]. To find P and Q, therefore, we need the inverse of this matrix, which is easily found to be

$$\begin{bmatrix} P+Q \\ P-Q \end{bmatrix} = \frac{1}{N} \begin{bmatrix} Bm_0 + \sum (Bd)\Lambda_{l,m} l'_0 & -\sum (Bd)\Lambda_{l,m} l_0 \\ -m'_0 - B \sum (Bd)\Lambda_{l,m} l_0 & m_0 \end{bmatrix} \begin{bmatrix} E(0) \\ E'(0) \end{bmatrix}, \tag{4.3}$$

where

$$\begin{aligned} N = {} & Bm_0^2 + \sum_{l\,(\neq m)} (Bd)\Lambda_{l,m}(m_0 l'_0 - l_0 m'_0) \\ & - B \sum_{l\,(\neq m)} \sum_{p\,(\neq m)} (Bd)^2 \Lambda_{l,m}\Lambda_{p,m} l_0 p_0\ . \end{aligned} \tag{4.4}$$

The last term in this expression contains two additional factors (Bd) and is thus much smaller than the other terms. It could thus have been dropped, but it was retained, however, to assure that the matrices in Eqs. (4.1) and (4.3) are each other's exact inverse. Once P and Q are known, the envelope function is completely determined [Eq. (3.13)]. To calculate the transmissivity of the linear stack now, we calculate the total electric field and its derivative at the front end of the structure, using Eq. (3.14), and match to the appropriate linear combination of a forward and backward traveling plane wave.

The merits of the procedure will now be illustrated by application to the linear stack under a simplifying approximation: taking φ_m to be associated with one edge of the lowest stop gap, we assume that only one coupling constant $\Lambda_{l,m}$ is significant, namely, that associated with the other eigenfunction bordering the same stop gap. This assumption is equivalent to the coupling assumed by Kogelnik in his analysis of distributed feedback lasers,[21] and we refer to it as the *Kogelnik approximation.* It means that only two plane waves—one propagating in the $+x$ direction and one propagating in the $-x$ direction—combine to form the Bloch states φ_m and φ_l. For a simple layer geometry we work out the Bloch functions in Appendix B; they are to be substituted into the equations in the beginning of this section. The Kogelnik approximation is known to be valid in the limit of small index differences between the constituent materials.[21]

We give the results for linear stacks with two different sets of parameters. In the first of these, the refractive indices of the constituents are 2.0 and 3.0. The other parameters of this stack are given in the caption of Fig. 2. It should be noted that $1/(Bd) \approx 17.3$ here, so Eq. (3.6) is satisfied. With such a large index difference, we expect the Kogelnik approximation to be rather unrealistic. Figure 2 compares the transmissivity which follows from the envelope approach to the exact results for a variety of lengths of the stack. Since the stack contains an integer number of periods, the exact results are a set of discrete points. As far as the envelope function is concerned, however, the stack can have an arbitrary length since, as we saw before [Eqs. (3.4) and (3.5)], the internal periodic structure disappears. For this reason the approximate results are given as a continuous curve. We see that the approximation is off by about 25% over the entire range of lengths. In spite of the large index difference, however, the results are qualitatively correct and even predict the rather subtle slope variations of the transmissivity.

In the next example, the index difference of the constituents is much smaller ($n_1 = 1.9$, $n_2 = 2.1$), and we expect the Kogelnik approximation to be valid. This second set of parameters thus represents a fairer test for the intrinsic properties of the envelope-function approach. We see from Fig. 3 that the approximate method works very well

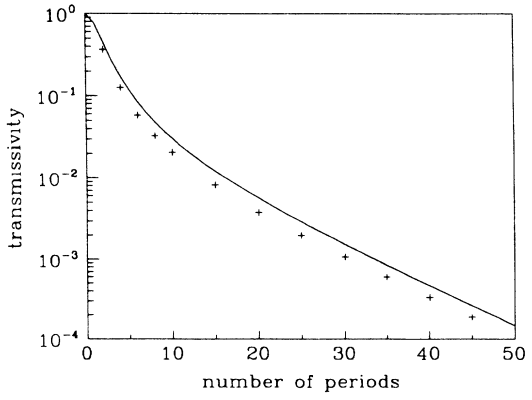

FIG. 2. Transmissivity following from envelope-function approach (solid line) compared to results from exact calculations (crosses), for linear stack with varying number of periods. For this example, $n_1 = 2.0$, $n_2 = 3.0$, and $d_1 = d_2 = 0.5$ μm. The wave number in the surrounding medium $k_s = 1.103\,33\ \mu\text{m}^{-1}$.

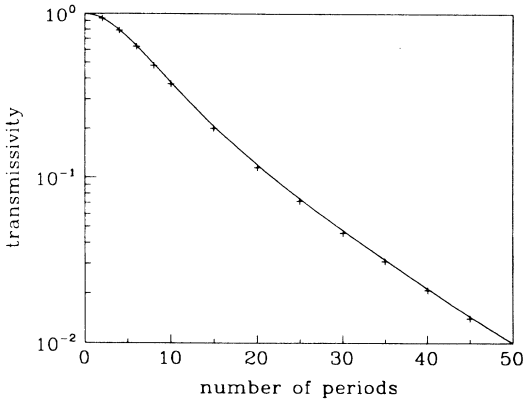

FIG. 3. Transmissivity following from envelope-function approach (solid line) compared to results from exact calculations (crosses), for linear stack with varying number of periods. For this example, $n_1=1.9$, $n_2=2.1$, and $d_1=d_2=0.1$ μm. The wave number in the surrounding medium $k_s=7.620\,00\ \mu\text{m}^{-1}$.

here, and that the deviations are only a few percent over the entire range of stack lengths. For this example, $1/(Bd)\approx 28.5$ so that, again, Eq. (3.6) is satisfied. Based on the results for the linear stacks, therefore, we conclude that the envelope-function approach gives satisfactory results in calculating the transmissivity. However, as emphasized in the beginning of this section, the real advantage of this method becomes much more clear in Sec. V, in which nonlinear stacks are investigated.

To finish this section we will rewrite these results for a linear stack such that a useful comparison to the solutions for the general nonlinear problem will be easiest. The idea is that, for vanishingly small nonlinearities, the general solution [Eqs. (3.19) and (3.23)] should be identical to that in terms of the simple exponential functions [Eq. (3.13)]. One connection between these two is provided for by Eqs. (3.15) and (3.22), which link W to P and Q. It is our aim to find a similar relation which links the parameter I_m to P and Q. In order to find such a relation it is important to notice that the square of the modulus of the general envelope function $I(z)$ has a maximum [Eq. (3.19)] or a minimum [Eq. (3.23)] at the origin. For this reason we will shift the envelope function for the linear stack in order to obtain a similar property. We thus calculate the square of the modulus of Eq. (3.13), I_L, and search for an extremal point x_0. Some algebraic manipulations show that

$$Bx_0=\tfrac{1}{2}\ln\frac{|Q|}{|P|}\ , \tag{4.5}$$

We now shift the origin by this amount and find

$$I_L(x)=(\sqrt{PQ^*}+\sqrt{QP^*})^2+4|P||Q|\sinh^2(Bx)\ . \tag{4.6}$$

This equation shows that the extremal point is, in fact, a minimum. Equation (4.6) is thus the linear limit of Eq. (3.23). We now rewrite this equation by introducing the angle between the arguments of P and Q, Θ_{PQ}. The result is then

$$I_L(x)=4|P||Q|\cos^2(\Theta_{PQ}/2)+4|P||Q|\sinh^2(Bx)\ . \tag{4.7}$$

To make the connection with the solutions of the general problem from Sec. III, we introduce I_m, which is here defined as the minimum value that $I_L(x)$ [Eq. (4.7)] can attain (this nomenclature reflects the results below),

$$\begin{aligned} I_m&=4|P||Q|\cos^2(\Theta_{PQ}/2)\ ,\\ W/B&=2|P||Q|\sin(\Theta_{PQ})\ , \end{aligned} \tag{4.8}$$

where the last line follows from Eqs. (3.15) and (3.22). We now rewrite Eq. (4.7) in terms of I_m and of W/B, and find that

$$I_L(z)=I_m+\left[I_m+\frac{W^2}{B^2I_m}\right]\sinh^2(Bz)\ , \tag{4.9}$$

which is the linear equivalent of Eq. (3.23). It should be mentioned that Eq. (4.9) can also be found by applying the limit in which $A\to\infty$ to Eq. (3.23) directly.

In Sec. V, Eq. (4.8) will be used extensively to investigate the relation between the boundary conditions for the linear and for the nonlinear stack. In doing so, it will be helpful to have a more explicit expression than Eq. (4.5) for the distance x_0 between the minimum of the envelope function and the boundary of the stack. The result can be written in a power series in Bd [$Bd\ll 1$, Eq. (3.6)]. For the present purposes, only the leading term of the series will suffice. Using Eqs. (4.3) and (4.4), it is found that

$$Bx_0=\frac{m_0dm_0'+\sum\Lambda_{l,m}dm_0'dl_0'+(k_sd)^2\sum\Lambda_{l,m}l_0m_0}{(dm_0')^2+(k_sd)^2m_0^2}\times(Bd)\ , \tag{4.10}$$

where k_s is the wave number of the radiation in the surrounding medium. Since, in applying Eq. (4.3), we have used the electric fields associated with an outgoing plane wave only, x_0 measures the distance between the minimum of the envelope function and the rear surface of the stack. The right-hand side of this equation is much smaller than unity. This can be demonstrated using an identical argument as in Section III, where it was shown that the principal term dominates the electric field [Eq. (3.8), and in following paragraph]. The result $|Bx_0|\ll 1$ will be crucial in Sec. V. It is no coincidence that we find a special relation between the position of the minimum and the rear surface, rather than the front surface, of the stack. As was mentioned earlier, the special footing of the rear surface is a consequence of the boundary condition with only an outgoing plane wave.

V. NONLINEAR FINITE STACK

After the preliminary work in Secs. II–IV, we now set out to find the properties of the general finite nonlinear stack. The energy flow will prove to be a significant parameter, since it determines the importance of the non-

linearity. It should be mentioned here that two different energy flows will enter the discussion. The first of these is the energy flow through the stack, which we will designate by S_1. The second, which we call S_0, is the energy emitted by an external source. This would be the control parameter in an actual experiment.

At a certain level this problem is quite straightforward. The functional form of the envelope function is well known, and, using Eq. (3.12), the entire field can be found everywhere in the stack for a given set of parameters. In principle, there are three such parameters: I_m, W, and also the relative position of the envelope function with respect to the stack. These parameters have to be determined in accordance with the boundary conditions at the rear surface of the stack, which prescribe the magnitudes of the electric field and of its first spatial derivative, and their relative argument. One of the three ensuing equations is unneccesary, however, since the energy flow, and thus W, is known, and we are left with two equations and two unknowns. To solve these, we have to search a two-dimensional space for a single solution. Actually, this procedure can be carried out quite easily, since the function of which we want to find the root [Eqs. (3.16)–(3.23)] can be calculated quickly. Such a procedure, however, turns out to be unnecessary, since the matching procedure for the linear stack can be applied to the nonlinear stack as well. This will now be shown.

It is clear that the envelope functions for the linear and for the nonlinear stack have quite different properties: Eq. (3.23), for the nonlinear stack, describes a periodic function, whereas Eq. (4.9), for the linear stack, does not. We will show, however, that (a) "sufficiently close" to the minima of these functions, the linear and the nonlinear envelopes have identical functional forms. This is only true, however, if the energy flow through the system S_1 is much smaller than a certain prescribed value S_L. After that we show, still only for $S_1 \ll S_L$, that (b) the rear surface is "sufficiently close" to the minimum. As far as the matching procedure is concerned, therefore, the linear and the nonlinear cases are identical. Finally, we show (c) that S_L is so large that the envelope-function approach itself breaks down long before this matching procedure does. The similarity between the linear and the nonlinear boundary conditions thus covers the entire regime in which the envelope function approach is meaningful. The proof of this somewhat surprising result consists thus of three parts, which will be given below.

We first show that the functional form of the linear and the nonlinear envelopes, close to the minima, are very similar, for an energy flow $S_1 \ll S_L$. In order to do so, we replace the functions appearing in Eq. (3.23) and in Eq. (4.9) by the first terms in their Taylor series expansions. We can do this by inspection for the hyperbolic function in Eq. (4.9). The expansion for the elliptic function in Eq. (3.23) is $\mathrm{cd}(x \mid k)=1-\frac{1}{2}(1-k^2)x^2+\cdots$.[18] Substituting this into Eq. (3.23), and using the definitions of I_+ and of I_- [Eqs. (3.21)], it is then found that

$$\hat{I}(x)=I_m+\left[I_m+\frac{W^2}{I_m B^2}\right]B^2x^2-2\left[\frac{I_m}{A}\right]^2 B^2x^2 , \tag{5.1}$$

where $\hat{I}$ was used to express the fact that this is an expansion for small arguments. Now compare this to the Taylor series expansion for the linear stack, following from Eq. (4.9). The first terms in Eq. (5.1) are seen to be identical to those in the expansion of Eq. (4.9). The final term in Eq. (5.1), however, does not have a linear counterpart, and, to lowest order, distinguishes the linear and the nonlinear envelope functions. As required, this term disappears in the linear limit of Eq. (5.1) ($A \to \infty$). Locally, the linear envelope function is thus a good approximation for its nonlinear counterpart, if

$$I_m+\frac{W^2}{I_m B^2} \gg 2\frac{I_m^2}{A^2} . \tag{5.2}$$

By Eqs. (4.8), I_m is proportional to the energy flow through the system, and, while the left-hand side of Eq. (5.2) is thus linearly proportional to S_1, the right-hand side is proportional to S_1^2. As expected, therefore, Eq. (5.2) will be satisfied if the energy flow is below a certain value S_L, the value for which the two sides of Eq. (5.2) are equal. To find an expression for S_L, Eq. (5.2) is rewritten as in equality in terms of the parameters of the stack, using Eqs. (4.8) and (4.3). This is quite straightforward, but very tedious; for this reason, only the final result is given here,

$$S_L=\frac{1}{4\pi c}\left[\frac{A}{Bd}\right]^2\frac{\omega_m\omega_m''}{(k_s d)^4} \times\left[\frac{(dm_0')^2+(k_s d)^2 m_0^2}{m_0^2+\sum\Lambda_{l,m}(m_0 dl_0'-l_0 dm_0')}\right]^3 . \tag{5.3}$$

It should be mentioned that Eq. (5.3) only gives the leading term in the expansion for S_L in powers of (Bd). As this equation depends on the ratio $A/(Bd)$ only, S_L is independent of the detuning [Eqs. (3.3)]. Once φ_m is selected, S_L is thus an intrinsic parameter of nonlinear stack. Also, $S_L \to \infty$ in the linear limit, as expected. This concludes the first part of our proof.

In the second part we assume that indeed $S_1 \ll S_L$, so that, close to the minima, the linear and the nonlinear envelope functions are very similar. We now include the rear surface into the discussion. We want to show that at a distance x_0 given by Eq. (4.10) from the minimum, the expansion leading to Eq. (5.1) is allowed. Since $|Bx_0| \ll 1$ [Eq. (4.10)], the expansion is certainly allowed for the linear envelope function in Eq. (4.9). We now use Eqs. (4.10) for Bx_0, and Eq. (3.22) to find an expression for the argument of the elliptic function in Eq. (3.23) at the rear surface of the stack. That argument is

$$\sqrt{I_+-I_-}\,\frac{B}{A}x_0=\left[\frac{3}{2}\right]^{1/2}\frac{1}{k_s d}\,\frac{m_0 dm_0'+\sum\Lambda_{l,m}dm_0'dl_0'+(k_s d)^2\sum\Lambda_{l,m}l_0 m_0}{m_0^2+\sum\Lambda_{l,m}(m_0 dl_0'-l_0 dm_0')} , \tag{5.4}$$

for $S_1 = S_L$. The right-hand side of this equation is of order unity. We thus conclude that, for $S_1 \ll S_L$, the field at the rear surface of the stack can be described accurately by the first terms of the Taylor series expansion of the elliptic functions.

We now turn to the third step of the proof in which we estimate the actual size of S_L. Obviously, if S_L turns out to be very small, the entire exercise is quite useless. An obvious way to estimate S_L is to substitute typical values into Eq. (5.3), but this is not satisfactory, since the dependence of S_L on A implies that we can give S_L any value by adjusting the nonlinear coefficient. A better approach is to relate S_L to the properties of the envelope function itself. We show that $S_1 \ll S_L$ whenever the envelope-function approach itself may be used. The envelope-function approach, in fact, is only valid when two distinct conditions are satisfied. First, as mentioned in Sec. III, the envelope function should vary slowly compared to the Bloch function. Also, in Sec. VI, we show that Eqs. (6.4) and (6.5) specify a second condition for the validity of our method. In the following paragraphs, we demonstrate that an energy flow as large as S_L implies that at least one of these two conditions is not satisfied.

As a start, we estimate the period of the nonlinear envelope function at S_L, to see if it is indeed slowly varying. The period of the elliptic function depends on the modulus k and we thus first have to find the value of this parameter at S_L. Using Eqs. (3.20) and (3.21), it is found that, in fact, the leading term in the expression for the modulus vanishes, and thus $k \ll 1$. Since for $k \to 0$, $\mathrm{cd}(x)$ is identical to $\cos(x)$, it is easy to find the period x_L of the envelope function in this limit,

$$\frac{x_L}{d} = \pi \left[\frac{2}{3} \right]^{1/2} (k_s d) \frac{m_0^2 + \sum \Lambda_{l,m} (m_0 d l_0' - l_0 d m_0')}{(d m_0')^2 + (k_s d)^2 m_0^2} . \tag{5.5}$$

This expression does not contain the parameters A and B; x_L is thus independent of the detuning and, more surprisingly, of the nonlinearity. The magnitude of the right-hand side of this equation is primarily determined by the coupling coefficients. Let us initially assume that none of these is much larger than unity, so that the same is true for the entire right-hand side of Eq. (5.5). Under this condition, therefore, the envelope function varies on the same length scale as the Bloch functions, and the envelope-function approach is thus invalid. We thus conclude that, when none of the coupling coefficients are much larger than unity, the envelope function approach is not valid at $S_1 = S_L$.

We now consider the opposite limit: we assume that one of the coupling coefficients is actually much larger than unity and calculate δ_{loc} as defined in Eq. (6.4). This is an effective local detuning which, according to the argument we present in Sec. VI, must be small enough to satisfy Eq. (6.5) for the envelope approach to be valid. Since this parameter depends on the magnitude of the envelope function, it varies throughout the stack. To show how large S_L actually is, we underestimate δ_{loc} by basing its calculation upon the lowest intensity in the stack I_m. We thus substitute Eqs. (4.3), (4.8), and (5.3) into Eq. (6.4), and find that

$$\frac{\delta_{\mathrm{loc}}}{|\omega_l - \omega_m|} \approx \frac{1}{(k_s d)^2} \left[\frac{[(d m_0')^2 + (k_s d)^2 m_0^2]}{m_0 d l_0' - l_0 d m_0'} \right]^2 , \tag{5.6}$$

for $S_1 = S_L$. The right-hand side of this equation is of order unity, so that, in this limit, Eq. (6.5) is violated. We thus conclude that, when a coupling coefficient is much larger than unity, the envelope function approach is not valid at $S_1 = S_L$ either.

We thus see that the envelope-function approach is never valid at $S_1 = S_L$, and thus, for energy flows for which the envelope-function approach is valid, the envelope functions for the linear and for the nonlinear stack are very similar close to the rear surface. The matching procedure for these two cases can thus be taken to be identical, without introducing significant errors. First, the parameters P and Q are thus found using Eq. (4.3). Then Eqs. (4.5) and (4.8) are used to find I_m and x_0. These parameters are then finally substituted into Eq. (3.23) to find the envelope function inside the entire nonlinear stack. Using Eq. (3.8), we now can find the electric field at the front surface of the stack, and thus also the transmissivity.

We will now first consider the field profiles in the nonlinear stacks. To start, we make a connection with the stationary soliton, found at the end of Sec. III. It should be stressed, however, that whereas the soliton only existed in the limit in which both $I_m \to 0$ and $S_1 \to 0$, the present solutions are associated with a nonvanishing energy flow. This difference is reflected by the fact that the present solutions are periodic, whereas the stationary soliton is not. However, when the period of the envelope function $x_s \gg 1/B$, then the distinction between the two is quite small. This behavior is illustrated in Fig. 4, in which the amplitude of the envelope functions are com-

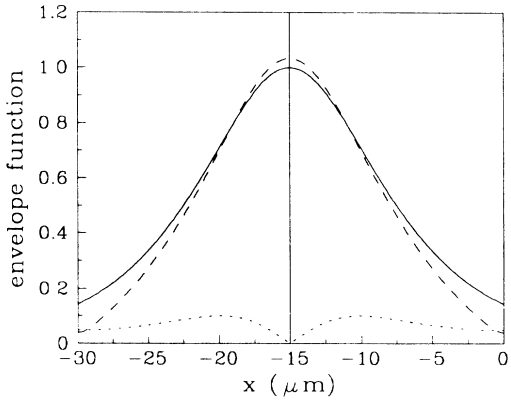

FIG. 4. Profiles of the envelope functions associated with the principal term (dashed line) and companion term (dotted line), compared to that of the soliton solution (solid line). For this example, the nonlinear stack has a uniform $\chi^{(3)} = -10^{-6}$ e.s.u. Furthermore, $n_1 = 1.9$, $n_2 = 2.1$, $d_1 = d_2 = 0.1$ μm, and $k_s = 7.62000$ $\mu\mathrm{m}^{-1}$. The Poynting vector is chosen such that the envelope function has a period of 150 stack periods.

pared to the soliton solution for a periodic stack with the same linear properties as the stack from in Fig. 3. Figure 4 was obtained using the Kogelnik assumptions which were discussed in Sec. IV and in Appendix B, with the details of the system specified in the figure caption. The energy flow was chosen such that the period of the envelope equals 150 stack periods. In this example $1/B \approx 27$ periods, so that the stack is much longer than the characteristic width of the soliton. It is seen from the figure that envelope function associated with the principal term (dashed line) follows the soliton envelope (solid line) quite closely, except at the edges. This is to be expected, since the minima of the actual envelope function at these positions do not occur for the envelope of the soliton. Furthermore, we know that the rear surface of the stack is close to one of these minima [Eq. (4.10)]. Consequently, the deviations from the solitonlike shape are largest at the rear surface of the stack, and at equivalent positions.

As the energy flow is increased, the envelope function grows taller and its period decreases. For this reason, the similarity between the actual envelope function and that of the soliton will grow worse with increasing Poynting vector. Qualitatively, however, the profile will not change much from that of Fig. 4, and, for this reason, no more field profiles will be presented. The decreasing similarity between the actual envelope function and that of the soliton, with increasing energy flow, is consistent with the general behavior of a resonance in a cavity.[20] The present situation of a nonvanishing energy flow is then analogous to that of a cavity with losses. It is well known that such losses introduce changes in the field profile, especially close to the cavity walls, and a shift and broadening of the resonance condition.[20] The present equivalent of the shifting resonance condition is the increase of I_+ with S_1 (Fig. 4). The increasing broadening with energy flow can be seen directly from Figs. 5–7, which we will discuss in detail below. Figure 4 also shows the magnitude of the envelope associated with the companion term (dotted line). As expected, its magnitude is much smaller than that of the principal term, except at the edges of the figure, or near the rear surface of the structure.

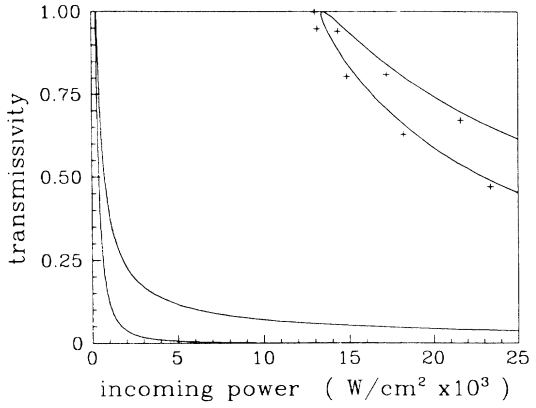

FIG. 6. Transmissivity vs incoming power S_0, for nonlinear stack with $n_1=1.9$, $n_2=2.1$, $d_1=d_2=0.1$ μm, $\chi^{(3)}=-10^{-6}$ e.s.u. uniformly, and a length of 200 stack periods. Furthermore, $k_s=7.625\,00\,\mu\text{m}^{-1}$.

We now turn to the calculation of the transmissivity of the nonlinear stack. To interpret the results of such calculations, let us first consider the transmissivity $\mathcal{T}$ as a function of the energy flow S_1 through the stack. The main features can be understood by the periodicity of the envelope function [Eq. (3.23)]. We expect some resonance effect when the period of the envelope function fits an integer number of times in the stack. Under this condition, the envelope function and its first derivative, and thus the entire electric field, attain identical values at the front and back surfaces of the stack. This implies that field at $x=0$ and $x=-L$ must be the same, and thus that the transmissivity then equals unity. This remarkable effect was found by Chen and Mills[5,6] in their numerical studies of nonlinear stacks. The transmissivity

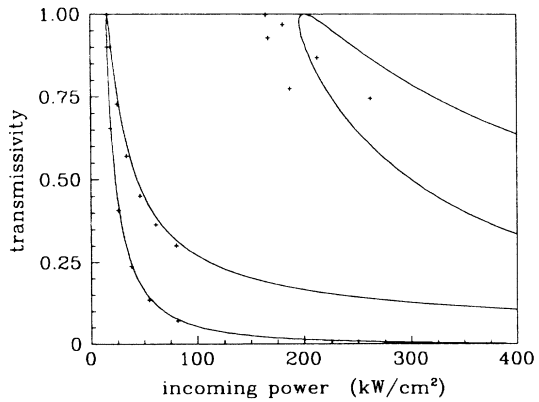

FIG. 5. Transmissivity vs incoming power S_0, for nonlinear stack with $n_1=2.0$, $n_2=3.0$, $d_1=d_2=0.5$ μm, $\chi^{(3)}=-10^{-4}$ e.s.u. uniformly, and a length of 80 stack periods. Furthermore, $k_s=1.103\,33\,\mu\text{m}^{-1}$.

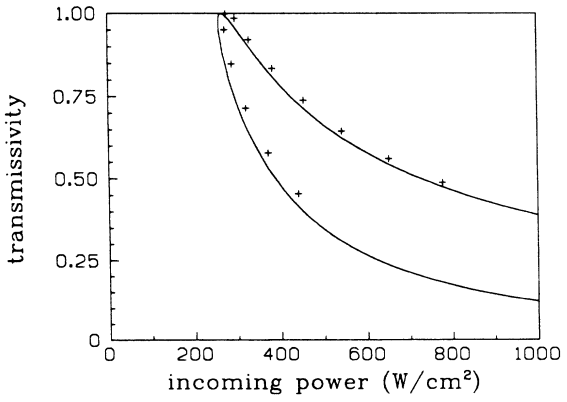

FIG. 7. Same as Fig. 6, but with expanded horizontal scale.

drops in between these resonances, but never to the level of the linear stack (except when $S_1 \to 0$).

Until now, we have only considered the properties of the nonlinear stack as a function of the energy flow through the stack S_1, which is the natural independent variable in the present problem. The control parameter in experiments, however, is the energy emitted by the source of radiation S_0. These two quantities are related by,

$$S_1 = \mathcal{T} S_0 \ , \tag{5.7}$$

where $\mathcal{T}$ is the transmissivity. Now consider $\mathcal{T}$ as a function of S_0. At the resonances, where $\mathcal{T}$ equals unity, $S_0 = S_1$. In between the resonances, however, S_0 is larger than S_1, the more so when $\mathcal{T}$ is small. To illustrate this behavior, and to judge the merits of the envelope-function approach, we refer to the Figures 5–7. These give the transmissivity as a function of the incoming power S_0 for two different nonlinear stacks. The linear properties of the stacks are identical to those of the examples of Sec. IV. The figure captions give the pertinent data. The results in Figs. 5–7 were obtained using the Kogelnik approximation mentioned in Sec. IV and in Appendix B. The approximate envelope results, found by the methods described in this section, are given by the solid lines in these figures; the exact results, from a numerical solution of the original equation [Eq. (2.3)] are indicated by the crosses. Indeed, S_0 grows rapidly in between the resonances; this behavior is so pronounced that we observe a markedly multivalued behavior of the transmissivity as a function of the incoming power. Such behavior was previously observed by Chen and Mills using numerical methods.[5,6]

Figure 5 shows the results for the stack in which the refractive indices of the constituents are quite different. It is clear that the envelope approach is qualitatively correct for this stack, but that the position of the resonances is not quite right. The deviation of the second resonance is much larger than that of the first one, which is not unexpected, since the energy flow for the two cases differs by about a factor of 10. Furthermore, because of the large index difference of the constituents, we expect our Kogelnik approximation to be quite unrealistic,[21] and the deviations are thus not surprising. Remember that the linear results for this stack exhibited deviations of about 25%.

The envelope-function approach is more stringently checked in Figs. 6 and 7, in which the index difference between the constituent materials is much smaller. Figure 7 has an expanded horizontal scale, to show the details of the first resonance. We saw in Sec. IV that the results for the linear stack were off by only a few percent. The first two resonances are seen to be quite well reproduced by the envelope-function approach. It should be mentioned, however, that the stack is rather long in this case (200 periods) and, in fact, is much larger than the width of the soliton ($1/B \sim 24$ periods). For the higher resonances the agreement between approximate and the exact results deteriorates quickly. This is not due to the Kogelnik approximation (see Sec. IV and Appendix B), but to intrinsic limitations of the envelope function method. A discussion of these limitations will be given in Sec. VI.

VI. DISCUSSION AND CONCLUSIONS

The approximations which were necessary to obtain the analytic results in Secs. II–V can be grouped into three different categories. The first of these is the application of the linear boundary conditions to the nonlinear stack. Secondly, we have made the Kogelnik assumptions (see Sec. IV and Appendix B), to simplify our calculations. Finally, we have intrinsic approximations associated with the use of the envelope method itself. In the current section, we will discuss these three sources of errors separately.

The first type of approximation is the use of the linear boundary conditions. A comparison with envelope function solutions based on the exact boundary conditions, mentioned in the second paragraph in Sec. V, shows that this approximation is excellent, and that the associated errors are negligible. This conclusion holds as long as the envelope-function approach itself is applicable. To understand this result, which was not initially expected, we should realize that the essence of the difference between the linear and the nonlinear stacks is that the nonlinearity provides a means to tune the radiation locally out of the stop gap of the structure. This behavior was discussed in the beginning of Sec. III, and will be quantified later in the present section. On the scale of the entire Brillouin zone, however, the detuning remains small, and thus $k \approx \pi/d$, throughout the stack, for our particular choice of φ_m. Since, moreover, the field and its first derivative at the rear surface are fully determined by the boundary conditions, we are led to conclude that in the region close to the rear surface, the electric field is virtually completely fixed by the boundary conditions and by our choice of φ_m, quite independent of the nonlinearity. We saw that, while $S_1 \ll S_L$, the minimum of the envelope function lies within this region, which implies that the linear boundary conditions can be used. Only at a certain distance from the rear surface, therefore, do the deviation from the value $k = \pi/d$ become relevant.

We now consider errors associated with the use of the Kogelnik approximation (see Sec. IV and Appendix B). Under this approximation only a single eigenstate φ_l was retained in the calculations. As discussed in Sec. IV, it is this assumption which is mostly responsible for the 25% error in Fig. 2. It is thus not surprising to find similar errors when a nonlinearity is introduced in the stack. Since the Kogelnik approximation is well understood,[21] and is not essential to our method, we will not discuss it further.

Finally, we thus consider the intrinsic approximations of the envelope-function approach. In a sense, these are quite obvious since the method is based upon an asymptotic series in which third and higher order terms, each made up of several contributions, were disregarded. To find among this myriad of neglected contributions the (few) relevant ones is more difficult. We have been able to identify two of these, which are discussed below.

The first relevant source of intrinsic error is Eq. (2.23) for the effective nonlinear coefficient of the stack. We see

that it only depends on the Bloch function φ_m and not on any of the other Bloch functions. Figure 4, however, shows that the companion term, which involves other Bloch functions than φ_m, can be comparable in size to the principal term. It would thus seem naive to expect that the effect of the nonlinearity could be described by a single coefficient α_m, depending on the Bloch function φ_m only. An obvious way in which this deficiency can be taken into account is to include the next highest term in the asymptotic expansion, Eq. (2.9). A discussion as in Sec. II shows that a term proportional to $\chi^{(3)}e_1^2e_2$, which would have the desired properties, is proportional to μ^4. Obviously, this source of error is absent in linear stacks.

The envelope-function approximation has at least one other relevant source of error, a problem related to the use of a simplified description of the dispersion curves. Notice that only ω_m and its first and second derivatives enter the discussion, whereas higher derivatives are disregarded. The dispersion curve in the vicinity of φ_m is thus approximated by a parabola. This description must fail for large values of the detuning, since Eq. (3.3b) predicts that the decay length will decrease monotonically with δ. We know this cannot be true indefinitely since the other edge of the stop gap is reached for $\delta = |\omega_l - \omega_m|$. Clearly, our description is only adequate close to the band edge corresponding to φ_m, or when

$$\delta \ll |\omega_l - \omega_m| \ . \tag{6.1}$$

This relation was satisfied in all our examples, and explains the good results for the linear stack with the small index difference. We conclude from Eq. (6.1) that the condition on δ becomes more restrictive when the stop gap shrinks, or, equivalently, when the index difference between the constituents of the stack decreases. To understand this in more detail, we turn to Eq. (A11), which gives the general expression for an element in the matrix representation of Eq. (A1). For a small index difference between the constituent, the stop gaps shrink and only the 2×2 part with the states $|m\rangle$ and $|l\rangle$ of the infinite matrix is relevant. We further take into account that these states have opposite parity, and find then

$$\begin{bmatrix} (\omega_m^2-\omega^2)+c^2q^2\langle m\mid m\rangle & 2cq\langle m\mid\Omega\mid l\rangle \\ 2cq\langle l\mid\Omega\mid m\rangle & (\omega_l^2-\omega^2)+c^2q^2\langle l\mid l\rangle \end{bmatrix} . \tag{6.2}$$

The definition of Ω in Eq. (2.15) assures that this matrix is Hermitian. The lowest-order corrections in q to the eigenvalues of this matrix are proportional to q^2, and this is the origin of our parabolic approximation. This perturbation expansion is only valid when the off-diagonal matrix elements are small compared to the difference between the diagonal elements. When the index difference of the constituents decreases, the stop gap shrinks, and so does the difference of the diagonal elements, restricting the validity of the parabolic approximation to smaller and smaller values of q.

As mentioned before, in our examples of linear stacks δ is chosen as to satisfy Eq. (6.1). Although this relation is well satisfied for the nonlinear stacks in Sec. V as well, the situation is now more complicated since, as discussed in Sec. III, the nonlinearity changes the local value of the detuning. Although Eq. (6.1) is satisfied, the local detuning in the regions with high intensity can be quite different than δ. For the subsequent discussion it is convenient to introduce the parameter $\delta_{\rm loc}$, which designates this value of the local detuning, as changed under the influence the nonlinearity. To get a quantitative measure of the local detuning, we rewrite Eq. (3.4) as

$$\psi'' - \left[-\frac{2}{\omega_m''}\delta\left[1-2\frac{|\psi|^2}{A^2}\right]\right]\psi = 0 \ , \tag{6.3}$$

where Eq. (3.3b) was used. The expression within the square brackets in this equation can be interpreted as a local value for B^2. Comparing Eq. (6.3) with the corresponding linear equation, we are led to define a local detuning $\delta_{\rm loc}$ to be

$$\delta_{\rm loc} = \left[1-2\frac{|\psi|^2}{A^2}\right]\delta \ . \tag{6.4}$$

To estimate the size of $\delta_{\rm loc}$ we should remember that the envelope function has a maximum value of $\sqrt{I_+}$, which equals A for $S_1=0$ (this was the soliton limit from Sec. III) and grows monotonically with increasing energy flow. In the soliton limit, therefore, $\delta_{\rm loc}=-\delta$ at maximum intensity, and the magnitude of $\delta_{\rm loc}$ thus never exceeds δ. In this limit we thus expect the parabolic approximation to be valid throughout the stack [if δ was chosen small enough to satisfy Eq. (6.1)]. With growing energy flow I_+ and the size of the third term in Eq. (3.4) increase and so, therefore, does the size of the local detuning. In this way, the nonlinearity can give us access to parts of the dispersion curve where the parabolic approximation is invalid, in spite of the fact that the detuning δ was chosen to be sufficiently small. Because of this, the nonlinearity forces us to introduce a more restrictive condition than Eq. (6.1), for the validity of the envelope function approach,

$$\delta_{\rm loc} \ll |\omega_l - \omega_m| \ . \tag{6.5}$$

For the two resonances shown in Eqs. (6) and (7), the energy flow is so small that I_+ is quite close to A^2. The local detuning, therefore, does not grow very much larger than δ, and, consequently, the parabolic approximation remains valid everywhere inside the stack. This is consistent with the good agreement of the results of the envelope-function approach with the exact results. For the third resonance, however, the deviations are significantly larger. We can understand this from the fact that $I_+ \approx 1.66A^2$ for this case, so that $|\delta_{\rm loc}| \approx 2.3$. For still higher values of the energy flow $|\delta_{\rm loc}|$ grows rapidly, rendering the parabolic approximation less and less useful.

In conclusion, we have presented an envelope function approach which leads to the nonlinear Schrödinger equation for the slow field component for an arbitrary nonlinear periodic structure. In investigating the solutions to this equation we have restricted ourselves to those with a harmonic time dependence and which are at rest in space,

and show that these can be expressed in terms of elliptic functions. We showed that, in applying the boundary conditions at the surfaces of the stack, the nonlinearity plays no significant role. This allows to find analytic solutions to the present problem. Our method gives good quantitative results for small values of the energy flow through the system; for higher values, however, the agreement deteriorates. The origin of this descrepancy, which we discussed in the present section, is the simplified description of the dispersion relations implicit in the method.

In addition to analytically predicting the multivalued transmissivity previously seen in numerical calculation, the envelope-function approach has allowed us to qualitatively understand the physics of such phenomena, and predicts the generality of such phenomena in one-dimensional nonlinear periodic structures. In this paper we have only begun to consider the nonlinear optics of such structures, restricting ourselves to stationary solutions of the equations. We plan to turn to the richer phenomena of pulse propagation in these structures in a future publication.

ACKNOWLEDGMENT

This work was supported in part by the Natural Sciences and Engineering Research Council of Canada, and by the Ontario Laser and Lightwave Research Centre.

APPENDIX A

In this appendix we derive expressions for the slope (i.e., group velocity) and the curvature (group-velocity dispersion), at a prescribed point of the dispersion curves of the linear stack. The equivalent procedure in solid-state physics makes use of the so called $\mathbf{k}\cdot\mathbf{p}$ method. In the application of the $\mathbf{k}\cdot\mathbf{p}$ method, one makes use of time-independent perturbation theory. In Sec. II we already alluded to the difference between the effective-mass (EM) eigenvalue equation [Eq. (2.5)] and the Schrödinger equation. It is this distinction that causes a difference in the application of perturbation theory to these two equations. This distinction, however, only shows up in the second- (and higher-) order corrections to the eigenfunctions. Since the present derivation requires only first-order corrections to the wave function, however, conventional perturbation theory can be applied straightforwardly. It should be stressed, however, that such a procedure can give rise to serious errors in other applications.

As is quantum mechanics, a small perturbation V is added to the eigenvalue equation [presently, Eq. (2.5)], so that it reads

$$(\mathcal{H}+\lambda V)\,|\,\psi\rangle=\epsilon\omega^2\,|\,\psi\rangle\ , \tag{A1}$$

where $\mathcal{H}=-c^2(d^2/dx^2)$ and ψ is a perturbed eigenstate. Under the influence of V, an eigenvalue ω_m^2 associated with an arbitrary unperturbed state $|\,m\,\rangle$ will change to

$$\omega^2=\omega_m^2+\langle\,m\,|\,V\,|\,m\,\rangle+\sum_{m'\neq m}^{\infty}\frac{|\,\langle\,m'\,|\,V\,|\,m\,\rangle\,|^2}{\omega_m^2-\omega_{m'}^2}\ . \tag{A2}$$

The $|\,m'\,\rangle$ in this equation refer to the other eigenfunctions $\varphi_{m'}$ of the unperturbed problem. We now apply Eq. (A2) to the dispersion curves associated with Eq. (2.5). We first observe that since the dielectric function $\epsilon(x)$ is periodic, the Floquet-Bloch theorem applies.[3] It states that the eigenfunctions φ_m can be written as

$$\varphi_m(x)=e^{ikx}u_{n,k}(x)\ , \tag{A3}$$

where $u_{n,k}(x)$ is periodic with the same period as dielectric function $\epsilon(x)$. The quantum numbers n and k are, respectively, equivalent to the band index and to the crystal momentum in solid-state physics. Substituting Eq. (A3) into Eq. (2.5) gives a differential equation for the functions $u_{n,k}(x)$, which reads

$$H_k u_{n,k}(x)=\omega_{n,k}^2\epsilon(x)u_{n,k}(x)\ , \tag{A4}$$

where the operator H_k is defined by

$$H_k=-c^2\left[\frac{d}{dx}+ik\right]^2\ . \tag{A5}$$

To find the slope and the curvature of band n at k, Eq. (4) is applied to a neighboring point in the Brillouin zone with crystal momentum $k+q$. This results in

$$(H_k+V_q)u_{n,\,k+q}(x)=\omega_{n,\,k+q}^2\epsilon(x)u_{n,\,k+q}(x)\ , \tag{A6}$$

where

$$V_q=-c^2\left[2iq\left[\frac{d}{dx}+ik\right]-q^2\right]\ . \tag{A7}$$

To proceed, perturbation theory is applied to Eq. (A6). Using Eq. (A2) leads to the following expression:

$$\omega_{n,\,k+q}^2-\omega_{n,k}^2=2cq\langle\,m\,|\,\Omega\,|\,m\,\rangle+c^2q^2\langle\,m\,|\,m\,\rangle+4c^2q^2\sum_{m'\neq m}\frac{|\,\langle\,m'\,|\,\Omega\,|\,m\,\rangle\,|}{\omega_m^2-\omega_{m'}^2}\ , \tag{A8}$$

to second order in q. The operator Ω is defined in Eq. (2.15). It is important to note that the matrix elements appearing in Eq. (A8) are those between the eigenfunctions φ_m, rather than those between the periodic functions $u_{n,k}$. The subscript m in this notation thus refers both to the band index n and to the crystal momentum k. From Eq. (A8) we can now immediately extract expressions for the group velocity ω_m' and the group velocity dispersion ω_m''. A straightforward calculation shows that

$$\frac{d\omega_m}{dk}\equiv\omega_m'=\frac{c}{\omega_m}\langle\,m\,|\,\Omega\,|\,m\,\rangle \tag{A9}$$

and

$$\frac{d^2\omega_m}{dk^2}\equiv\omega_m''=\frac{c^2}{\omega_m}\langle\,m\,|\,m\,\rangle-\frac{(\omega_m')^2}{\omega_m}+\frac{4c^2}{\omega_m}\sum_{m'}\frac{|\,\langle\,m'\,|\,\Omega\,|\,m\,\rangle\,|^2}{\omega_m^2-\omega_{m'}^2}\ . \tag{A10}$$

The summation in the last term on the right-hand side of Eq. (A10) includes, in principle, all states $m'\neq m$. As in solid-state physics, however, the periodicity of the struc-

ture imposes a conservation law of crystal momentum[3] which causes all matrix elements with $k \neq k'$ to vanish, so that only a summation over the band index remains. Equations (A9) and (A10) are the final results of this appendix. They are used in Sec. II in the application of the method of multiple scales.

At this point it is important to mention that Eq. (A8) could have been found as well by applying Eq. (A7) to Eq. (A1) directly. To show this we write the perturbed state $|\psi\rangle$ in Eq. (A1) as $\sum a_m |m\rangle$, where the summation is over the band index,[10] and project onto each of the eigenstates $|m'\rangle$. This gives rise to a square matrix of infinite order. An arbitrary element $M_{m'm}$ in this matrix can be written as

$$M_{m'm}=(\omega_{m'}^2-\omega^2)a_{m'}\delta_{m'm}+2cq\langle m'|\Omega|m\rangle a_m + c^2q^2\langle m'|m\rangle a_m \ . \tag{A11}$$

Applying standard perturbation theory to a matrix with these elements then immediately yields the perturbation expansion in Eq. (A8). Equation (A11) is used in Sec. VI, where it is applied to the present problem in which φ_m is chosen to be at the edge of the Brillouin zone. The definite parity of the Bloch functions then prescribes that the second term in Eq. (A11) vanishes if the two states have the same parity. The third term, on the other hand, vanishes if the parity of the two states is opposite.

APPENDIX B

The general equations in the present paper are illustrated by applying them under a set of specific limiting conditions. Under these conditions, we concentrate on the lowest stop gap (see Fig. 1) and neglect the influence of the states associated with the higher gaps. This implies that only two states enter the discussion (the states at the upper and lower edge of the gap) so that the sum over l [as in Eq. (2.12)] consists of just a single term. In this limiting case, our treatment is equivalent to the approach of Kogelnik for the analysis of distributed feedback lasers. In order to work out a concrete example, we have to make some additional choices. First, we will identify φ_m with the lower edge of the lowest stop gap and φ_l with the upper edge. In addition, the first layer of the stack is chosen to have the low index of refraction, whereas the last layer has a high index. Finally, the layers of the constituent materials are assumed to have equal thickness. These assumptions fully specify the Bloch functions of the stack. Since the Bloch functions φ_m and φ_l are located at the edge of the Brillouin zone, they have a period of $2d$, where d is the period of the constituent materials. We thus conclude that

$$\sqrt{L}\,\varphi_m=n_c\cos\left[\frac{\pi}{d}x-\frac{\pi}{4}\right], \qquad \sqrt{L}\,\varphi_l=n_s\sin\left[\frac{\pi}{d}x-\frac{\pi}{4}\right], \tag{B1}$$

where the coefficients n_c and n_s are still to be determined. The origin of the coordinate x is at the rear of the stack and points to the medium behind the stack (cf. Fig. 4). The phase of $\pi/4$ has been included in Eq. (B1) to assure that the Bloch functions will peak at the correct positions. The eigenfunction associated with the lower edge of the stop gap φ_m peaks in the middle of the high-index material, whereas the other eigenfunction φ_l will do so in the middle of the layers with the low refractive index. The parameters n_c and n_s follow from the normalization conditions in Eq. (2.5),

$$n_c=\frac{1}{\left[\frac{1}{4}(n_2^2+n_1^2)+\frac{1}{2\pi}(n_2^2-n_1^2)\right]^{1/2}}, \qquad n_s=\frac{1}{\left[\frac{1}{4}(n_2^2+n_1^2)-\frac{1}{2\pi}(n_2^2-n_1^2)\right]^{1/2}}, \tag{B2}$$

where we made the choice that $n_2>n_1$. In Secs. IV and V we show that the Bloch functions only enter the discussion explicitly when applying the boundary conditions at the two surfaces of the stack. Consequently, only the values and the first derivatives of φ_m and φ_l at the origin will be needed in the calculations.

[1] M. Born and E. Wolf, *Principles of Optics,* 6th ed. (Pergamon, London, 1980), Chap. 1.

[2] H. A. Macleod, *Thin Film Optical Filters* (Hilger, London, 1969).

[3] N. W. Ashcroft and N. D. Mermin, *Solid State Physics* (Holt, Rinehart and Winston, New York, 1976).

[4] H. G. Winful, Appl. Phys. Lett. **46**, 527 (1985).

[5] Wei Chen and D. L. Mills, Phys. Rev. Lett. **58**, 160 (1987).

[6] Wei Chen and D. L. Mills, Phys. Rev. B **36**, 6269 (1987).

[7] D. L. Mills and S. E. Trullinger, Phys. Rev. B **36**, 947 (1987).

[8] J. E. Sipe and H. G. Winful, Opt. Lett. **13**, 132 (1988).

[9] R. K. Dodd, J. C. Eilbeck, J. D. Gibbon, and H. C. Morris, *Solitons and Nonlinear Wave Equations* (Academic, London, 1982).

[10] J. M. Luttinger and W. Kohn, Phys. Rev. **97**, 869 (1955).

[11] For a review see, e.g., IEEE J. Quantum Electron. **QE-22**, 9 (1986).

[12] See, e.g., G. Bastard, Phys. Rev. B **24**, 5693 (1981).

[13] K. O. Hill, Y. Fujii, D. C. Johnson, and B. S. Kawasaki, Appl. Phys. Lett. **32**, 647 (1978).

[14] Y. R. Shen, *The Principles of Nonlinear Optics* (Wiley, New York, 1984), Chap. 3.

[15] H. W. Wyld, *Mathematical Methods for Physics* (Benjamin, London, 1976), Chap. 2.

[16] Wei Chen and D. L. Mills, Phys. Rev. B **35**, 524 (1987).

[17] P. F. Byrd and M. D. Friedman, *Handbook of Elliptic Integrals for Physicists and Engineers* (Springer, Berlin, 1954).

[18] *Handbook of Mathematical Functions,* edited by M. Abramowitz and I. A. Stegun (Dover, New York, 1970), Chap. 16.

[19] In the definition of the modulus of the elliptic functions we have adopted the same convention as Ref. 17.

[20] J. D. Jackson, *Classical Electrodynamics,* 2nd ed. (Wiley, New York, 1975), Chap. 8.

[21] H. Kogelnik, Bell Syst. Tech. J. **48**, 2909 (1969).